

Numerical investigation of the dynamic response of lathe steel waste concrete subjected to blast loading

Olawale S¹, Ofuyatan O², Omeje M³

¹Department of Civil Engineering Faculty of Engineering and Environmental Sciences Osun State University, Osogbo, Nigeria

²Department of Civil Engineering Covenant University, Ota Ogun State

³Department of physics Covenant University, Ota Ogun State

Corresponding author-olatokunbo.ofuyatan@covenantuniversity.edu.ng

Abstract : The current work investigates the blast resistance capability of lathe steel waste composite concrete (LSWCC) using finite element numerical analysis. The static compressive, tensile and flexural strength of the composite concrete at varying percentages of lathe steel waste were experimentally determined. The static compressive strength for concrete with lathe steel waste percentage between 0% and 2% by weight at increment of 0.5% varies between 24.45MPa to 29.7 MPa with the maximum value of 35.93MPa at 1.5% of lathe waste contents. The dynamic numerical analysis shows clearly that lathe steel waste reduces the displacement considerably and the peak values of acceleration, velocity, shear force and moment occurred at 1.5% volume fibre content.

Keywords:- lathe steel, blast loading, dynamic response, numerical, concrete

1. Introduction

Concrete has good compressive strength and weak in tension. Addition of fibre into concrete improves its matrix composition with the provision of confinement to the molecular structure leading to improved performance in tension and shear. In dynamic realm, the response of composite concrete has not been exhaustively investigated because of the complexity of experimental methodology. However, numerical computation using finite element method of analysis has proven to be useful for the prediction of the dynamic response of composite concrete structural elements. This is necessary because of the incessant terrorist attacks across the continents and more particularly in the developing world like Nigeria.

Although a lot of work has been carried out on steel scrap reinforced concrete under static loading but not much has been done on the dynamic response. It is imperative for more work to be done to establish how Steel scrap reinforced concrete will behave under blast loading. Conventional concrete is highly brittle and suffers total damage under blast loadings

[1], [2]. Generally, the addition of dispersed short fibrous materials into concrete matrix is a way to improve survivability of concrete structures in a blast environment [3],[4], [5] carried out experiments on a one way simply supported and a two way steel fibre-reinforced concrete (SFRC) panels under varying blast loads. The panels were reinforced with hooked end steel fibre at fibre content ranging from 0.5% to 1.5% and aspect ratios varying between 33 and 75. The panels were subjected to hemispherical blast waves from detonation of varying trinitrotoluene (TNT) charge weight. They reported that SFRC panels exhibited improved damage tolerance to blast loading. It was also observed that as the fibre content increased from 0.5% to 1.0%, there was a reduction in the residual displacement. Similar observations using SFRC slabs were reported by [6] and they noted that 1.0% fibre concentration is optimum in resisting damage. In addition, they concluded that long fibre performed better than the short fibre in resisting cracking and spalling. [7] concluded that spiral-shaped steel fibres added to concrete matrix improved the compressive strength, post-failure strength and high energy absorption capacity.

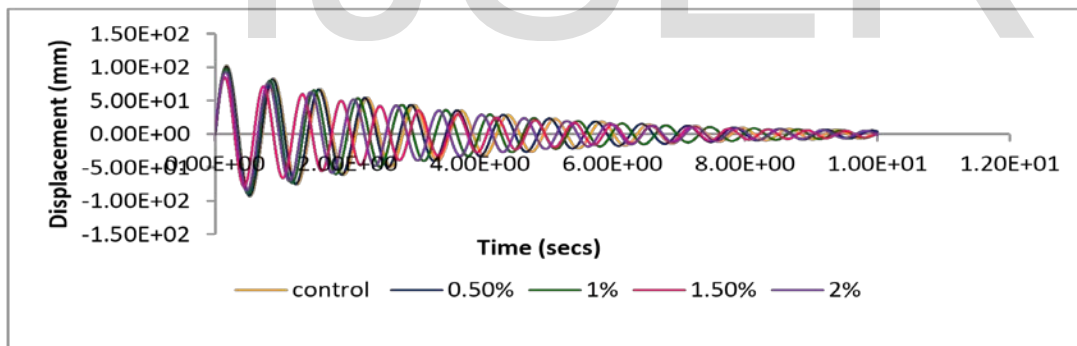
Several investigations into the effects of blast loadings on concrete, including both experimental and numerical studies have been reported in the open literature [8], [9], [10], [11], [12]. The aim of this work is to investigate the dynamic behavior response of lathe steel waste concrete using finite element method with the experimentally determined dynamic strength characteristics.

2. Experimental method

2.1 Material and mix proportions

Locally available Portland Cement Type II conforming to ASTM-C192 was used. Natural River sand of maximum particle size of 3.18mm was used as fine aggregates and crushed granite (maximum size of 12mm) obtained from local quarries as coarse aggregates. Portable water free from salts was used for casting and curing of concrete. Lathe steel waste fibres were obtained from the machining process of the lathe machine. The fibre was mixed at varying percentages with concrete matrix of 1:2:4 design mix. Concrete specimens were cured for 28 days before tested.

2.2 Numerical method



A dynamic finite element method was used in

analyzing the LSWCC beam of 3m long, with cross-section dimension of 100mm x 200mm. An elastic approach was employed with non-linear behavior accounted for in the form cracked concrete stress strain curve. The time response solution is traced using direct integration approach. Java computer programming language was used to develop the main classes.

3.0 Results and discussion

The compressive strength was determined for each percentage of lathe steel waste (0%, 0.5%, 1.0%, 1.5% and 2.0% %) by weight of cement. Table 3.1 presents the compressive strength and percentage increase with respect to plain concrete (0%) while Figure 3.1 shows the influence of fibre content on compressive strength.

Table 3.1: Compressive Strength test result of varying percentages of fibre

Fibre content %	No	Mass (Kg)	Density (Kg/m ³)	average density	Load at failure (KN)	Compressive strength (N/mm ²)	Average strength (N/mm ²)	% increase
0	1	8.4	2488.9	2479.01	563.1	25.03	24.45	0
	2	8.3	2459.3		576.2	25.6		
	3	8.4	2488.9		511.4	22.7		
0.5	1	8.35	2474.1	2464.19	546.5	24.2	25.13	3
	2	8.3	2459.3		517.4	22.9		
	3	8.3	2459.3		632.6	28.12		
1	1	8.45	2503.7	2449.38	598.4	26.59	27.47	12
	2	8.4	2488.9		653.7	29.05		
	3	7.95	2355.6		602.4	26.77		
1.5	1	8.4	2488.9	2493.83	824.6	36.64	35.93	47
	2	8.45	2503.7		797.5	35.44		
	3	8.4	2488.9		803.5	35.71		
2	1	8.4	2488.9	2489.27	763.9	33.95	29.7	21
	2	8.4	2488.8		608.6	27.04		
	3	8.45	2503.7		632.3	28.1		

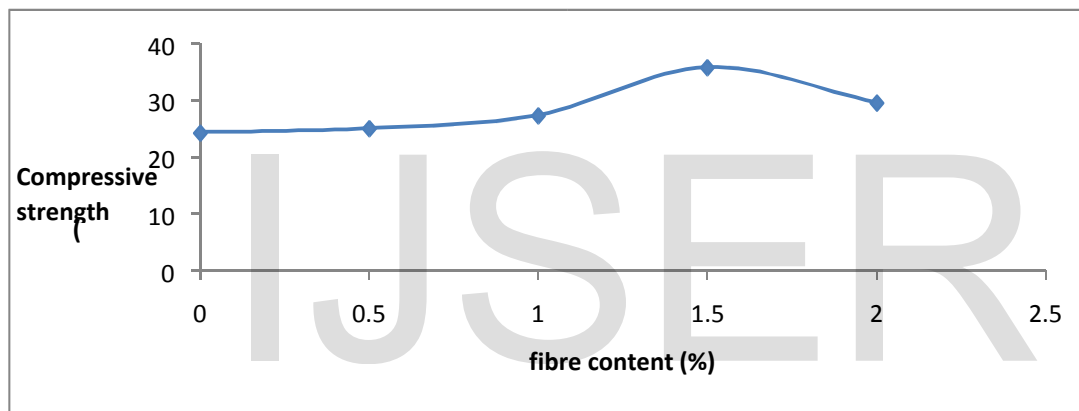


Fig.3.1: Influence of varying fibre content on compressive strength.

Compressive strength increased with addition of fibre by 47%, however, it later decreased with higher fibre content 2%). This may be caused by creation of air voids because of the relatively high fibre content.

3.2 Dynamic modulus of elasticity computation

The computation of dynamic modulus of elasticity is based on the method proposed by [13] and the results and computation as shown in table 3.2.

Table 3.2 Static and Dynamic Modulus of Elasticity.

s/no	V_f (%)	$\frac{l_f}{d_f}$	f'_c (Mpa)	density (kg/m ³)	ϵ_0	E_{static} (Mpa)	$E_{dynamic}$ (Mpa)
M1	0	75	24.45	2479.01	0.002641	19109.86	22931.83
M2	0.5	75	25.13	2464.19	0.002815	20264.24	24317.09
M3	1	75	27.47	2449.38	0.003013	20563.19	24675.83
M4	1.5	75	35.93	2493.83	0.003285	22449.26	26939.11
M5	2	75	29.70	2489.27	0.003379	20293.89	24352.67

3. Numerical Analysis of Dynamic Response

Program Validation

In order to validate the current dynamic finite element analytical tool developed, a 3m concrete beam of cross section dimensions of 200 mm depth and 100

mm breadth. The beam is simply supported and a constant dynamic load of 500 KN was applied at the mid-span. Hand computation of the same beam using two elements was carried out and the results obtained from the present program and hand computed ones are presented in table 3.3. The agreement between the hand and program computed results is excellent.

Table 3.3: comparison of Hand Computation with the java program.

S/N	Time (sec)	Hand Computation			Computer Results		
		Dis (m)	Vel (m/s)	Acc (m/s ²)	Dis (m)	Vel (m/s)	Acc (m/s ²)
0	0	0	0	1041.5	0	0	1040
1	0.003	0.00469	3.123	1040.99	0.00468	3.12	1040
2	0.006	0.01874	6.242	1039.44	0.0187	6.23	1040
3	0.009	0.04214	9.532	1036.87	0.0423	9.34	1040
4	0.012	0.07485	12.443	1033.27	0.0748	12.4	1030
5	0.015	0.1168	14.908	1028.65	0.116	15.5	1030

The results for compressive strength, density and dynamic modulus of elasticity obtained for the different fibre contents in the static tests were

imputed into the code developed to generate the time history for displacement, shear force, velocity, acceleration and moment.

3.4 Displacement-Time History

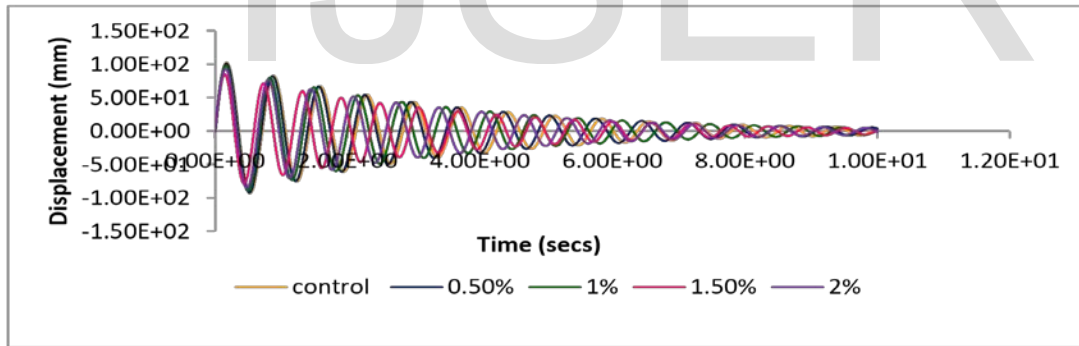


Fig.3.2: Comparison of displacement for LSWCC of varying fibre content.

As shown in fig 3.2 a realistic blast wave through a displacement-time history measured on a simple beam element. Here the typical characteristics of a shock wave become visible. The blast load is characterized through a shock front at the beginning of the load

followed by an exponential decay within the positive phase followed by the negative phase. The sampling rate chosen is very high in order to get high-precision results. Table 3.5 below presents the percentage increase in displacement as fibre content increases.

Table 3.5 Displacement variation with increasing fibre content

%	Max.displacement(mm)	% increase
0	9.39E+01	0
0.5	9.58E+01	2.015017
1	9.30E+01	-0.91805
1.5	8.19E+01	-12.7824
2	8.99E+01	-4.23771

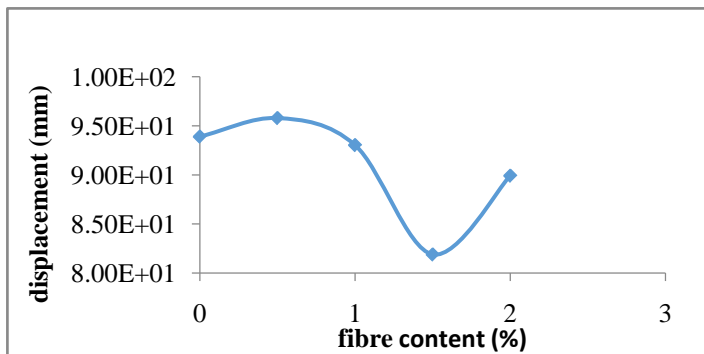


Fig.3.3: Displacement variation as fibre content increases.

In Figure 3.3 an increase in displacement is observed as fibre content increased from 0%

to 1.5% followed by slight increase as fibre content decreased from 1.5% to 2.0%.

3.5 Shear Force-Time History

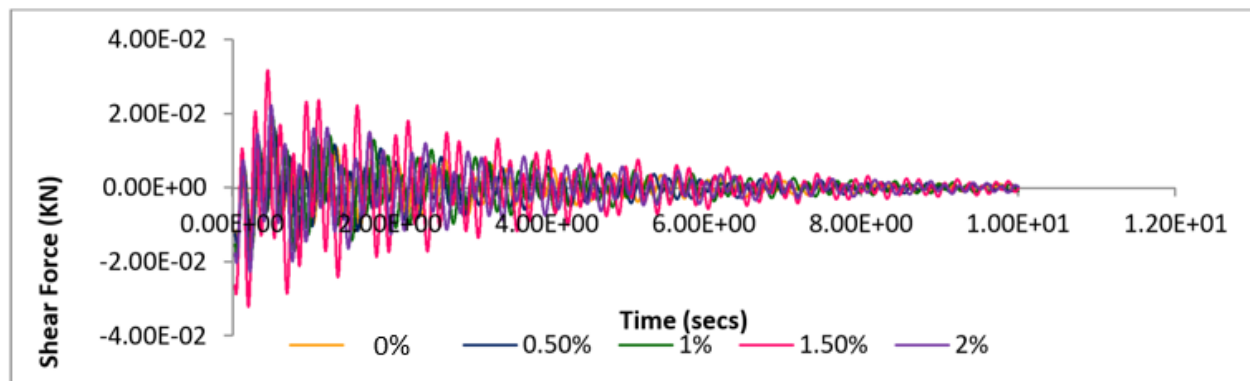


Fig.3.4: Comparison of shear force for LSWCC of varying fibre content.

Figure 3.4 shows a realistic blast wave through a force-time history measured on a simple beam element. Here the typical characteristics of a shock wave become

visible. Table 3.6 below presents the percentage increase in shear force as fibre content increases.

Table 3.6 Shear Force variation with increasing fibre content

(%)	max shear force (KN)	% increase
-----	----------------------	------------

0	1.42E-02	0
0.5	1.60E-02	12.67606
1	1.79E-02	26.05634
1.5	3.05E-02	114.7887
2	2.11E-02	48.59155

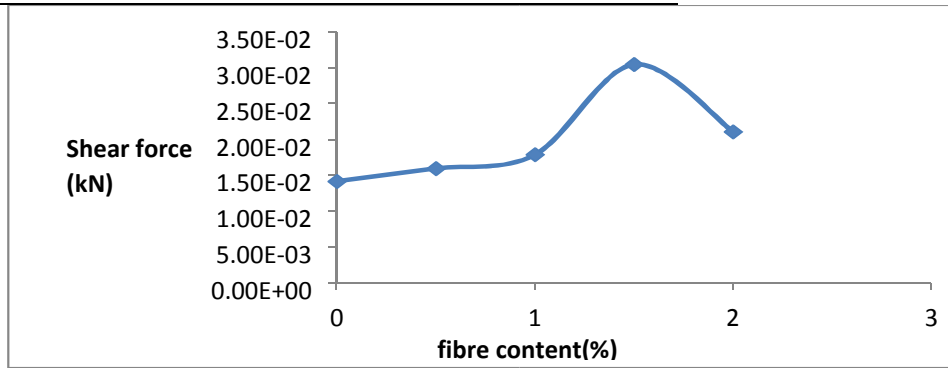


Fig.3.5 Shear Force variation as fibre content increases

In Figure 3.5 an increase in shear force is observed as fibre content increased from 0% to 1.5% followed by slight increase as fibre content decreased from 1.5% to 2.0%.

3.6 Velocity-Time History

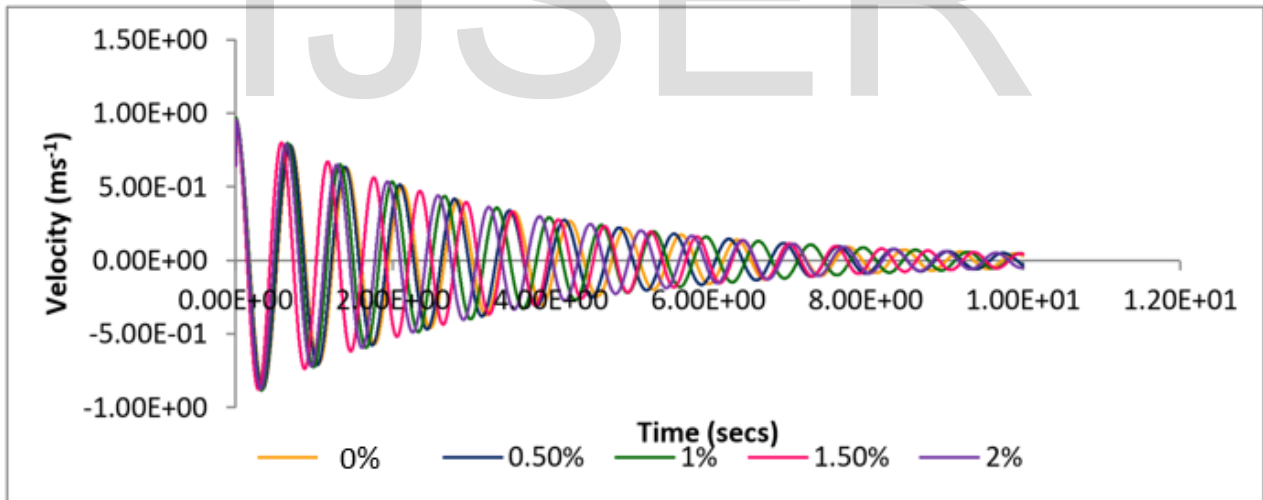


Fig.3.6 Comparison of velocity for LSWCC of varying fibre content.

Figure 3.6 shows a realistic blast wave through a element. Table 4.6 below presents the percentage increase in velocity as fibre content increases.

Table 3.7 Velocity variation with increasing fibre content

(%)	max velocity (ms ⁻¹)	% increase
0	7.34E-01	0
0.5	7.96E-01	8.440284

1	7.54E-01	2.758931
1.5	7.65E-01	4.169051
2	7.43E-01	1.215292

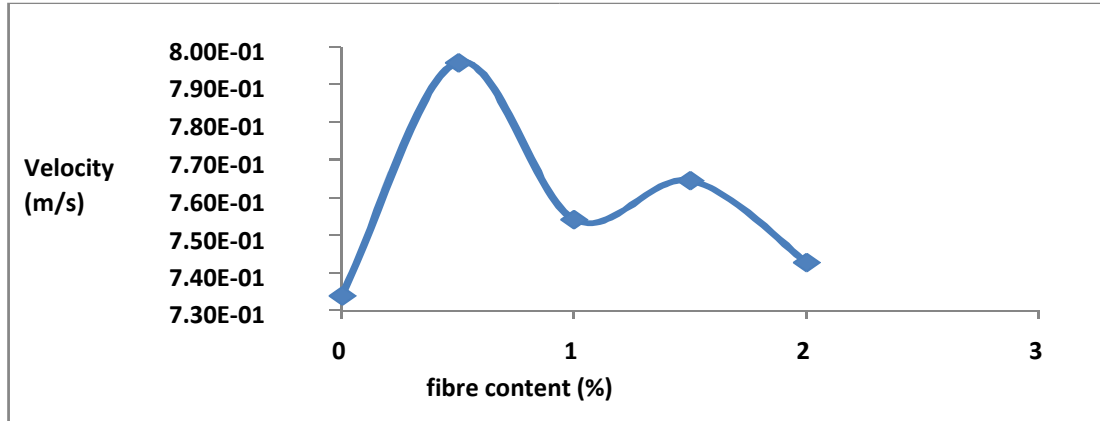


Fig. 3.7 Velocity variation as fibre content increases

In Figure 3.7 an increase in velocity is observed as fibre content increased from 0% to 0.5% followed by

slight decrease as fibre content increased from 1.0% to 2.0%.

3.7 Acceleration-Time History

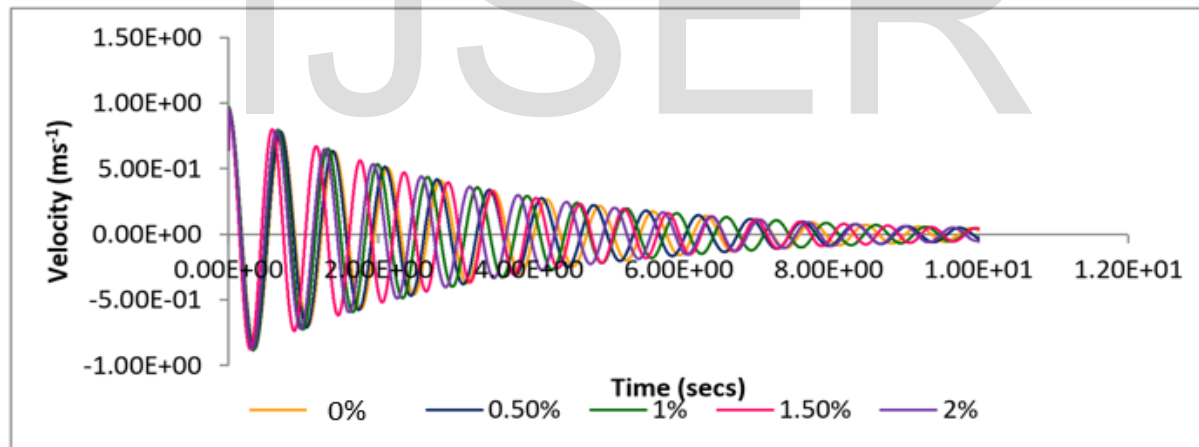


Fig.3.8: Comparison of acceleration for LSWCC of varying fibre content.

Figure 3.8 shows a realistic blast wave through an acceleration-time history measured on a simple beam element. Here the typical characteristics of a shock wave become visible. The blast load is characterized through a shock front at the beginning of the load

followed by an exponential decay within the positive phase followed by the negative phase. The sampling rate chosen is very high in order to get high-precision results. Table 4.7 below presents the percentage increase in acceleration as fibre content increases.

Table 3.8 Acceleration variation with increasing fibre content

(%) Maximum acceleration (ms^{-2})	% increase (%)
---	----------------

0	2.32E-02	0
0.5	2.47E-02	6.277969
1	2.94E-02	26.52324

Fig. 3.9 Acceleration variation as fibre content increases.

In Figure 4.9 a reduction in acceleration is observed as fibre content increased from 0% to 1.5% followed

by slight increase as fibre content increased from 1.5% to 2.0%.

3.8 Moment-TimeHistory

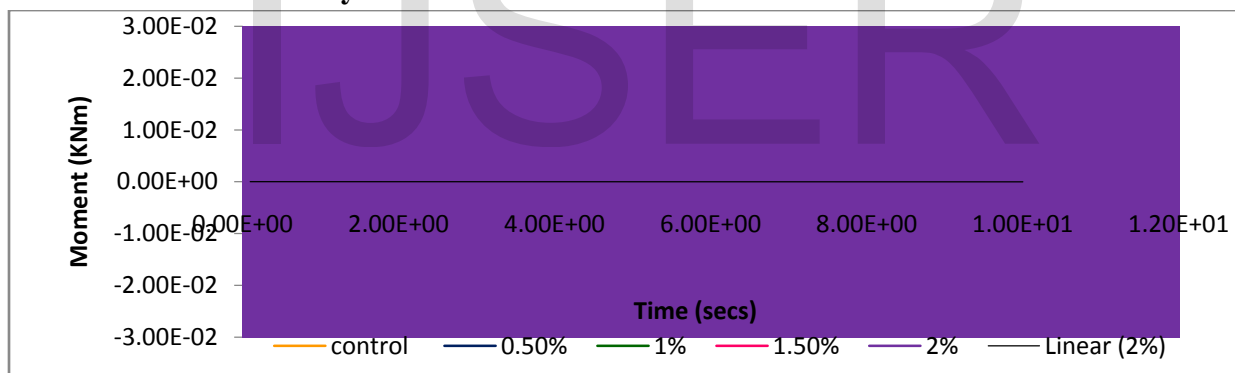


Fig. 3.10 Comparison of moment for LSWCC of varying fibre content.

Figure 3.10 shows a realistic blast wave through moment-time history measured on a simple beam element. Here the typical characteristics of a shock wave become visible. The blast load is characterized

through a shock front at the beginning of the load followed by an exponential decay within the positive phase followed by the negative phase. The sampling rate chosen is very high in order to get high-precision results. Table 3.9 below presents the percentage increase in moment as fibre content increases.

Table 3.9 Moment variation with increasing fibre content

V_f (%)	max moment (KNm)	% increase (%)
0	1.02E-02	0
0.5	9.98E-03	-2.53906
1	1.22E-02	19.53125

1.5	1.86E-02	81.44531
2	1.24E-02	20.60547

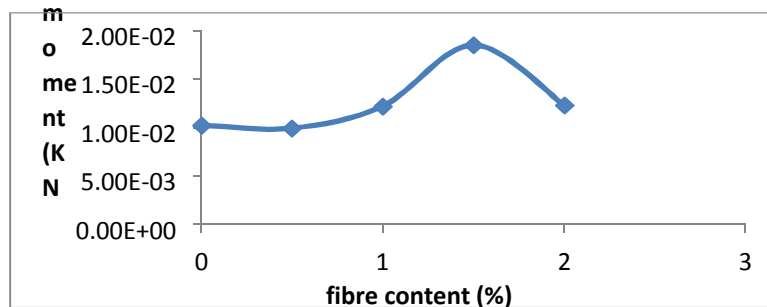


Fig. 3.11 Moment variation as fibre content increases

Figure 3.11 shows that increase in moment is observed as fibre content increased from 0% to 1.5% followed by slight increase as fibre content increased from 1.5% to 2.0%.

4. CONCLUSION

Laboratory and numerical analysis have been performed to investigate the compressive strength and dynamic properties of Lathe steel waste composite concrete (LSWCC). The dynamic properties analysed are displacement, shear force, velocity, acceleration and moment of LSWCC beams. These properties are also compared with those of plain concrete. The considered fibre contents are 0.5%, 1.0%, 1.5% and 2.0% for 40mm long fibres. Three specimens of LSWCC were tested for each combination of fibres to get reliable average results.

The static investigation reveals the properties can increase or decrease depending on content, and LSWCC strengths can be greater or smaller than that of plain concrete. The testing confirmed that lathe

steel waste in concrete can improve its compressive strength considerably for all considered cases. The following conclusion can be drawn from the parametric study from the numerical simulation of dynamically loaded lathe waste composite concrete beams by using the central difference scheme for the numerical analysis. To make as accurate calculations as possible, the material properties have to be defined based on the actual behaviour of lathe waste and concrete. The dynamic tests show that damping of LSWCC beams has, as expected, grown and the fundamental properties have declining trend with increasing time. The increase of fibre content has resulted in a higher damping ratio. LSWCC beams with 0.5% fibre content have higher damping as compared to those with other fibre contents. The static and dynamic modulus of elasticity increases with an increase in fibre content. From the considered cases, LSWCC with 0.5% fibre content has the best overall mechanical and dynamic properties. The results of the present study shows that it is possible to predict the response of dynamically loaded LSWCC beams.

REFERENCE

- [1] Li, J., &Hao, H (2013). Influence of brittle shear damage onaccuracy of two-step method in prediction of structural response to blast loads. *International Journal of Impact Engineering*, 54, 217-231
- [2] Li, J., &Hao, H. (2014). Numerical study of concrete spall damage to blast loads. *International Journal of Impact Engineering*, 68, 41-55.

- [3] Mutalib, A.A., &Hao, H. (2011). Development of P-I diagrams for FRP strengthened RC columns. *International Journal of Impact Engineering*,38, 290–304.
- [4] Wu, C., Oehlers, D.J., Wachl, J., Glynn, C., Spencer, A., Merrigan, M., &Day,I. (2007). Blast testing of RC slabs retrofitted with NSM CFRP plates. *Advances in Structural Engineering*, 10, 397–414.
- [5] Xiao, J.R., &Lok, T.S. (1999). Steel-fibre-reinforced concrete panels exposedto air blast loading. *Proceedings of the ICE – Structures and Buildings*, 134,319–331.
- [6] Lan, S., Lok, T. S., &Heng, L. (2005). Composite structural panels subjected to explosive loading. *Construction and Building Materials*, 19, 387 – 395.
- [7] Xu, Z., Hao, H., & Li, H. (2012). Experimental study of dynamic compressiveproperties of fibre reinforced concrete material with different fibres. *Materials & Design*, 33, 42–55.
- [8] Silva, P. F. and Lu, B., (2009). Blast resistance capacity of reinforced concrete slabs, *Journal of StructuralEngineering* vol. 135(6): 708-708.
- [9] Tai, Y. S., Chu, T. L., Hu, H. T. and Wu, J. Y., (2011). Dynamic response of a reinforced concrete slab subjected to air blast load, *Theoretical and Applied Fracture Mechanics* 56(3): 140-147.
- [10] Wang, W., Zhang, D., Lu, F., Wang, S. and Tang, F., (2013). Experimental study and numerical simulation of the damage mode of a square reinforced concrete slab under close-in explosion, *Engineering Failure Analysis* 27: 41-51.
- [11] Zhao, C. F. and Chen, J. Y., (2013). Damage mechanism and mode of square reinforced concrete slab subjected to blast loading, *Theoretical and Applied Fracture Mechanics* 63-64: 54-62.
- [12] Pantelides, C. P., Garfield, T. T., Richins, W. D., Larson, T. K. and Blakeley, J. E., (2014). Reinforced concrete and fiber reinforced concrete panels subjected to blast detonations and post-blast static tests, *Engineering Structures* 76(0): 24-33
- [13] Seong-Cheol Lee, Joung-Hwan O. and Jae-Yeol Cho (2015) Compressive Behavior of Fiber Reinforced Concrete with End-Hooked Steel Fibres” *Materials* 2015, 8, 1442-1458; doi:10.3390/ma8041442.